# Characterization of the Effects of High Intensity Negative Current Pulses on Metal Transfer and Melting Rate in the AC-GMAW Process

**Alisson Fernandes da Rosa** ( alissonaula@gmail.com )
UFSC: Universidade Federal de Santa Catarina https://orcid.org/0000-0001-6369-8790
**Luciano Machado Cirino**
**Claudio Marques Schaeffer**
**Mateus Barancelli Schwedersky**
**Regis Régis Henrique Gonçalves e Silva**

**Research Article**

**Keywords:** Variable Polarity, AC-MIG, Pulsed GMAW, Complex Waveform

**Posted Date:** June 21st, 2022

**DOI:** https://doi.org/10.21203/rs.3.rs-1742042/v1

# Abstract

The use of variants of the GMAW process has become an affordable option in industry. Alternating current Gas Metal Arc Welding (AC-GMAW) arises as one of them, providing additional degrees of freedom for process controllability and versatility. This study focused on the analysis of a complex waveform of the AC-GMAW process for welding stainless steel, employed in modern synergic programs, which has not been widely disseminated in the technical literature and assessed scientifically. The main objective was to characterize the effects of high intensity pulses in negative polarity over the process and to discuss the potential of this strategy, since it has not been used in conventional AC synergic programs. In order to bring to light information on the phenomena involved, such as the arc climbing on the wire electrode, advanced techniques of high-speed videography were used, synchronized with the acquisition of electrical welding process signals, as well as infrared thermography, to verify the evolution of the cooling of the piece after welding. The results grounded discussions on different AC-GMAW waveforms. The process´s electrical data, along with images of the arc and analysis of the wire melting and workpiece thermal behavior, showed that there was a significant visible increase in wire melting during the negative pulse. In addition, it evidenced how the negative electrode increment contributed to the increase in wire melting even at lower power and also showed the thermal effects on the workpiece.


# 1. Introduction

The evolution of the electronic control of welding power sources has made it possible to develop several variations or modalities of the gas metal arc welding (GMAW) process in recent decades. The simplest and probably most widespread example is pulsed GMAW. This basically consists of imposing a current signal that alternates between a lower current level sufficient to maintain the arc and keep the end of the electrode in the liquid state and a higher level aimed at the formation and detachment of a metal drop. This approach provides greater versatility of the process, overcoming the limitations imposed by conventional GMAW welding power sources, especially with respect to metal transfer modes (short-circuit, globular and spray). In short, GMAW with current pulsing allows metal transfer without contact between the wire and the workpiece (spray), but with an average current typical of metal transfer with contact between the wire and the workpiece (short-circuit or globular) [1]. The most cited advantages are the possibility of welding out of the flat position, spatter reduction, greater penetration, and a weld bead with a more adequate geometry, or better wettability, especially when welding materials such as stainless steels and aluminum alloys [2].

In recent years, there has been a profusion of GMAW process modalities developed by various manufacturers (e.g., STT, RMD, ColdArc, Cold MIG, CMT and MicroMIG). Kah et al. [3] give a detailed description of these and other modalities, where the authors argue that although the innovations are designed to meet industry demands they are not always used to their full potential due to a lack of deeper understanding. One such process is variable polarity GMAW, for which there is no consensus as to the most appropriate designation and the term AC-GMAW (alternating current - gas metal arc welding) is used in this article. The aim of this process is to combine the desirable characteristics of pulsed GMAW

(controlled metal transfer) and of negative polarity GMAW (direct current electrode negative – DCEN). The most widespread advantage of DCEN polarity is the higher melting rate of the electrode wire and lower heat input to the workpiece. Although these characteristics are well documented, they are still subject of discussion and are assessed herein.

The DCEN welding process has been described as a reversal in the balance of energy that is transferred to the electrode and the workpiece [4–5]. More specifically, in DCEN polarity, it is generally reported that 70% of the arc energy is transferred to the electrode and the rest to the workpiece. This feature may be desirable from a productivity standpoint, however, conventional GMAW in the DCEN condition is considered to be very unstable, subject to excessive spatter formation, with droplet repulsion, low penetration and low wettability weld beads, along with being limited to the globular metal transfer mode [6]. Souza et al. [7] demonstrated that with the use of a suitable gas mixture (98% Ar + 2% $O_2$), a stable transfer without droplet repulsion and with low spatter is obtained for steel wires. However, low wettability persists. Furthermore, was employed two average current values (150 A and 250 A) and observed that the metal transfer remains globular at 150 A [7]. Thus, it appears that the stable DCEN condition is limited to high average currents, for example, above 250 A, which in practice makes it impossible to weld thin sheets or perform welds in out-of-flat positions.

However, disregarding the energy balance, the higher melting rate in the DCEN condition is generally attributed to the phenomenon of arc climbing in the solid extension of the wire electrode [8]. This behavior is characterized by the action of the arc over much of the solid extension of the electrode, which causes a kind of preheating and this is responsible for the higher melting rate compared to the same process operating only in the direct current electrode positive (DCEP) mode under the same conditions. This is mainly due to the arc ‘seeking’ the oxide layer present on the surface of the electrode, which is known to facilitate electron emission and arc maintenance. Yarmuch e Patchett [9] cite that the predominant type of emission is cathodic emission, a phenomenon that produces more energy at the cathode, thus increasing the melting rate. Souza et al. [7] noted that the higher melting rate in DCEN is due to the higher thermal efficiency of the arc over the area of the electrode as it ‘seeks’ oxides for cathodic emission, rather than the heat generated in the arc and wire connection.

# 1.1 AC-GMAW waveforms and EN ratio

The expansion in the number of new modalities of the arc welding process is driven by the possible combinations of different transfer modes, for example, welding programs that impose a certain number of transfer cycles using controlled short-circuit interspersed with cycles of free flight transfers typical of a pulsed waveform. It is also common for each of the major equipment manufacturers to name their waveform using an acronym or a name with good commercial impact. In addition to the distinction between the waveforms, it is possible to adopt different control strategies to change the way the metal drop is transferred from the wire to the molten pool, thus offering different options for each type of material and application. Inserted in this context, the AC-GMAW, process based on the control of the current waveform, was conceived to take advantage of the two polarities, positive (DCEP) and negative

(DCEN). Initially, this modality was presented as a solution for thin plate welding. Tong et al. [10] and Rosa et al. [11] showed the ability of the process to fill the root in overlapping joints formed by aluminum sheets, when there is an irregularity or a large gap between them, and they used the term gap bridging ability. Harwig et al. [12] explored this same ability, however, for carbon steel-base materials. Joseph [13] showed that the process can be applied in a dissimilar welding process using galvanized steel with aluminum alloys. There are also studies that consider the application of AC-GMAW to thick plates Arif e Chung [14] and for single-pass butt-joint welding of structural steel AH36 [15], filler welding in butt joints with an aluminum "V" groove for the marine industry [15] and cladding of boiler walls with nickel alloy [8]. Kang et al. [17] used AC in GMAW Tandem welding with two wires, to mitigate the harmful action of the magnetic field generated between the two arcs, stabilizing the metal transfer and increasing productivity. The versatility of this process allows for studies in the area of advanced manufacturing that investigate the benefits of AC-GMAW, focusing on the adjustment of welding parameters based on real-time sensing and feedback control [18]. In addition, the reduced heat input that AC-GMAW offers compared to DC-GMAW, contributes to the control of the microstructure formed and allows for dissimilar welding between aluminum and hot-dip galvanized steel, which promotes evaporation of zinc (Zn) layer and formation of brittle Fe-Al intermetallic compound (IMC) layer can affect the joint quality both thermally and metallurgically [19].

However, most applications use the traditional AC-GMAW waveform, which incorporates only a current threshold in negative polarity, bounded by the parameters of negative current ($I_n$) and negative time ($t_n$) (Fig. 1.a). In general, the aim of the negative phase is to increase the melting rate and reduce heat input to the workpiece without compromising the process stability, since droplet detachment occurs in a controlled manner during the positive stage. Another approach to this mode features a more complex waveform. This was firstly proposed by Japanese companies that incorporated an additional negative current pulse ($I_p$–) into the negative polarity together with the base threshold ($I_b$–) found in traditional AC-GMAW waveforms. Arif and Chung [20] stated that this approach is primarily aimed at further increasing the wire electrode melting rate. Jaskulski [21], on the other hand, states that the negative pulse helps bringing the arc back to an acceptable spatial stability during the inherently unstable EN phase. In any case, this advanced waveform (Fig. 1.b) is used only for steels, while the traditional AC-GMAW waveform (Fig. 1.a), with only a plateau on the negative side, is still used by the same manufacturers for aluminum alloys [22]. Both shapes in Fig. 1 were used in the study reported herein.

To support the discussions in this paper, a schematic drawing of the complex waveform was prepared and is shown in Fig. 2. A legend has been inserted in the Table 1 to show the meanings of the various parameters and thresholds of the current waveform used in this study.

Table 1
Meaning of the complex waveform thresholds corresponding to Fig. 1.

| | | | |
|---|---|---|---|
| **t +:** | **Time current remains in positive polarity** | **$t_p$+:** | **Duration of the positive current pulse** |
| t −: | Time current remains in negative polarity | $t_b$+: | Duration of the positive current base |
| tc: | Duration of one current cycle | $t_p$−: | Duration of the negative current pulse |
| tic: | Initial time of one current cycle | $t_b$−: | Duration of the negative current base |
| tfc: | Final time of one current cycle | $I_p$+ | Current Intensity of the positive pulse |
| | | $I_b$+ | Current Intensity of the positive base |
| | | $I_p$− | Current Intensity of the negative pulse |
| | | $I_b$− | Current Intensity of the negative base |

Following the development of modern synergic programs, despite the considerable number of parameters involved, welding equipment operators do not necessarily need an in-depth understanding of the role of each parameter. The study and development of parameterization is not within the scope of this study, but this is addressed in, for instance, [8–23–24]. However, although there are some similarities, it should be noted that the cited authors consider totally rectangular waveforms. Also, the melting rate needs to be proportional in the two polarities in order to obtain a constant arc length and the determination of the negative electrode percentage (%EN) is based on the negative time ($t_n$). This is useful for setting parameters, but the %EN may be insufficient for evaluating the effects of negative polarity on the weld bead and the piece to be welded in advance. This is due to the fact that the %EN often only takes into account times and does not consider current values ($I_n$). However, in some cases, the performance of the negative electrode can be represented under different strategies and this merits further attention to estimate the effects of negative polarity on the welding process. Tong et al.[10] and Rosa et al. [11] also considered the current values and adopt this approach when defining what is called the EN ratio. In a simplified way, and considering a rectangular waveform, Harwig et al. [12] and Park et al. [25] used Eq. 1 to estimate more accurately the EN ratio.

$$\mathbf{ENRatio} = \frac{(I_n . t_n)}{(I_p . t_p) + (I_b . t_b) + (I_n . t_n)} \quad \text{(Eq. 1)}$$

Basically, Eq. 1 represents the ratio between the negative phase area (DCEN) and the total area enclosed by the entire welding current signal in one cycle (DCEN + DCEP), as shown in Fig. 2. It is important to highlight that because the electrical signals of the process with alternating current vary between positive and negative polarity, it is necessary to use absolute values so that the different signals are rectified and can be summed to give an overall average. However, even calculated in absolute values, the results for

average voltage and average current may present some limitations in relation to the calculation of the power dissipated in the conductor with the application of non-symmetric waveforms and the average signal value will still be inaccurate. Thus, in this study, we employed (and highlight the importance of) the true root mean square (or true RMS) value, which is used when it is necessary to measure alternating current with waveforms that are not necessarily constant over time. Thus, the measuring device performs a mapping of the wave, point by point, marking these points and calculating the average at that particular instant, since the current and voltage were captured at an infinite number of instants in a given period of time. Eq. 2 shows the calculation performed by the electrical signal acquisition system and this was used to calculate both the current and voltage values. The values for these electrical signals are represented by $X_{RMS}$, the period in each cycle is T as a function of time (t).

$$\mathbf{X_{RMS}} = \sqrt{\frac{1}{\mathbf{T}}\int_{0}^{\mathbf{T}} \mathbf{X}^2(\mathbf{t}).\,\mathbf{dt}} \qquad \text{(Eq. 2)}$$

Furthermore, considering the representation in Fig. 2, Equations 3 and 4 show mathematical representations of the calculation of the average current values for the positive and negative polarities, respectively. These calculations can be used to verify, in isolation, the effect of the welding current on only one polarity if needed.

$$\mathbf{DCEP} = \int_{\mathbf{tic}}^{\mathbf{tfc}} \mathbf{I} > 0\mathbf{dt} \qquad \text{(Eq. 3)}$$

$$\mathbf{DCEN} = \int_{\mathbf{tic}}^{\mathbf{tfc}} \mathbf{I} < 0\mathbf{dt} \qquad \text{(Eq. 4)}$$

Thus, if the percentage of negative polarity is calculated based on the DCEP and DCEN values, from Equations 3 and 4, respectively, it is possible to obtain the appropriate EN ratio, through Eq. 5.

$$\mathbf{ENRatio} = \frac{\mathbf{DCEN}}{\mathbf{DCEN} + \mathbf{DCEP}} \qquad \text{(Eq. 5)}$$

Therefore, within the context of technological advances as well as the scarcity of visual results in the literature, an analysis and discussion of the welding process, focused on the effects of negative polarity in the wire electrode are provided herein and constitute the objective of the present work. The practical aspects related to the use of the EN ratio in AC-GMAW are also described. This discussion is supported by analysis of macrographs, the electrical parameters of welding and high-speed footage, as well as infrared thermal monitoring of the workpiece. The waveform used in modern synergic systems for welding stainless steels (Fig. 2.b) is evaluated, especially with regard to the effect of using an additional pulse in the negative polarity of the process and, consequently, the influence on the resulting weld. In addition, the performance obtained with different percentages of negative electrode in this complex waveform is also explored.

# 2. Materials And Methods

In the present study, it was necessary to use two different welding power sources. To generate the traditional AC-GMAW waveform (Fig. 1.a) an IMC-Digiplus A7 welding power source was used, assisted by software that allows the current waveform to be designed according to the desired application and considering the most common materials used industrially. To study and understand the complex waveform (Fig. 1.b), which employs two current steps in negative polarity ($t_p–$, $I_p–$), the OTC Daihen-DW300 welding power source with the synergic software for welding stainless steels was used. In this case, different percentages of negative electrode (EN ratios of 30%, 60% and 50%), based on Eq. 5, were also used during the evaluation of the effect of additional negative current pulses ($I_p–$) on the wire electrode and analysis of the macrographs. To evaluate the cooling profile by means of thermal filming under the workpiece and to extend the potential of the study with regard to this aspect, in addition to those mentioned above, two additional intermediate EN ratios were used (i.e., 40% and 65%).

During all the tests, the wire AWS 5.9/ER309LSi with 1.2 mm diameter and a gas mixture in the proportion $Ar + 2\%O_2$ at a flow rate of 15 $l.min^{-1}$ were used. The welding performed was of the bead-on-plate type, using SAE 1020 carbon steel with 9.6 mm thickness, and the displacement of the welding torch was performed mechanically, using a robotic welding manipulator SPS/Tartilope-V2 with motorized shaft that allows a constant speed and distance between the contact nozzle and the workpiece to be maintained. To monitor the process, the experiment was conducted using a portable electrical signal acquisition system IMC-SAP.v4, that calculates the average values of the current and voltage signals according to the methodology in Eq. 2, at a sampling rate of 5 kHz and with a measurement uncertainty of 2%. To better visualize the effects of the arc, two cameras specifically for monitoring arc welding processes were used. The analysis of the thermal effects under the workpiece with different EN ratios was performed with an FLIR-SC7200 camera and the analysis of the effects of the negative current pulses on the electrode wire was performed using an IDT-Y4S2 MotionPro high-speed camera at an image acquisition rate of 4166 fps (frames per second) assisted by laser illumination (Cavilux-HF) to minimize the luminosity coming from the electric arc in the image obtained. In the evaluation of the weld bead geometry, two samples for each case were selected, cut cross-sectionally and metallographically prepared. Chemical attack was then performed by immersing the sample surface in 4% Nital chemical reagent for 10 s. Figure 3 shows a schematic diagram of the experimental bench.

# 3. Results And Discussion

# 3.1 Metal transfer and waveform features

Figure 4 was assembled from frames of high-speed footage taken during the AC-GMAW welding of stainless steel. Below the images is a current and voltage oscillogram synchronized to a specific frame. In image (a) the process is in the negative base current ($I_b–$, $t_b–$) with a value of -41 A, for the purpose of keeping the arc open, as with the base current in the positive polarity in image (f). In image (a) (c) and (f)

it is not possible to see the arc, because, since the objective of the filming was to register the metal transfer, the laser illumination was regulated in such a way as to diminish as much as possible the luminosity coming from the arc. However, the effects of the arc heat on the wire are visible, showing the melting potential during these moments. Image (b) corresponds to the negative pulse ($I_p$–, $t_p$–) that, in fact, was able to increase the melting rate of the process, as seen in image (c), and also ensured the maintenance of the arc at the moment of polarity variation, especially with very high percentages of negative electrode, due to the rapid rise of the current signal. At this instant, it is possible to see that the current reverses abruptly from the value of approximately − 300 A to 450 A, which corresponds to a variation of 750 A in just 1 ms. No harmful or unwanted fading of the arc during the procedure was identified from the images acquired at a high rate (4166 fps) or from the current and voltage oscillograms. Jaskulski [21] states that this approach allows negative electrode percentages of up to 80% to be achieved with less risk of arc extinction in polarity reversal. The strategy of using a pulse with high current was also important in providing the extra function of ensuring sufficient and adequate penetration even using alternating current, besides providing increased wire fusion at this time, offered by the negative polarity, for carbon steel or stainless steel. As can be seen, the current ($I_p$–) exceeds − 300 A and in this case the arc is clearly visible. Even using an improved laser illumination system, the arc intensity is still too high for this current level. It is thus evident that the climbing of the arc toward the free extension of the wire electrode causes melting and influences the detachment of the metallic droplet. The visible contribution in increasing the melting of the free extension of the wire electrode can be explained by the higher efficiency of heat transfer from the arc to the electrode in negative polarity, mainly by increasing the contact surface between the two. However, in the tests performed it was found that, although the current pulse in negative polarity presents relatively high intensity and duration (400 A and 3 ms, respectively), the current concentration is not sufficient, at a given point of the wire electrode, to promote sufficient pinch effect (Lorentz Force) for droplet detachment during this period. The droplets were detached only in the positive current pulse, in a regular and stable way, as shown in images (d) and (e). In the conventional P-GMAW welding process (positive polarity only), the strategy is generally drop detachment in the current pulse, as this provides more control, besides delivering deeper weld penetration when compared, for example, to drop detachment in the base time. In the present study, the drop detachment at the end of the positive pulse was repeated in all situations analyzed, thus eliminating the possibility of metal transfer during a high current pulse in the negative polarity.

To gain a better understanding of the role of the pulse in negative polarity, results for three negative electrode conditions (30, 50 and 60%) are presented. The graph in Fig. 5 was prepared using three current signals obtained and superimposed to highlight that there is no notable difference on the positive side of the waveform ($I_b$+, $t_b$+, $I_p$+, $t_p$+) between the different EN ratios used. However, there is a difference on the negative side of the current waveform ($I_b$–, $t_b$–, $I_p$–, $t_p$–). In addition, the figure highlights the moment immediately after the negative pulse (before the start of the positive pulse) for each of the three conditions tested. It can be seen that as the EN ratio increases, the length of the molten wire electrode tip prior to the positive pulse is also greater, reaching a length of up to 4 mm. Initially, it is possible to infer that the higher percentage of negative electrode, in fact, has a very significant effect, and provides a

greater amount of molten wire in each cycle. In this case, it is important to note that as this ratio increases, the frequency of the positive pulses (and, consequently, the detachment frequency) strongly decreases. Thus, larger droplets must be transferred in each positive pulse. It is known that when designing the waveform in the GMAW-P process, the metal droplet diameter should approach the diameter of the wire used [26]. The waveform with an EN ratio of 60% resulted in a theoretical droplet diameter of approximately 1.67 mm, which is 47% larger than the wire diameter. In addition to favoring the occurrence of secondary droplets during metal transfer, the large increase in the droplet volume could explain the increase in the occurrence of spatter that was observed for this condition. This means that with an increase in the percentage of negative electrode, i.e., an increase in the melted region of the free extension of the wire electrode, the arc length or the distance between the contact tip and the workpiece needs to be manipulated, these being factors of extreme importance for the regularity of the process. This was consistently observed in the present study through high-speed filming.

Figure 6 shows the unwanted effects when the highest percentage of negative electrode was used. The frames taken from the high-speed film are represented in the graph in this figure. In image (1) it is possible to verify the moment of the short-circuit, where excessive volume of the molten droplet combined with the small distance between the electrode and the workpiece are responsible for the beginning of the unstable condition of the process. In (2), the welding source increases the current value to promote sufficient pinch effect to detach the droplet. This behavior causes instability in the process, which can be seen by the elimination of the negative base step ($t_b$–) in the next instant. This characteristic may represent the control strategy of the synergic program of the welding power source, whereby, even with severe instability in the process, the power source acts as to keep the waveform period (the negative pulse was maintained, in this case). In image (3) it can be observed that there is a short-circuit with a duration so short that the source does not detect, or does not react to, the contact by reading the current signal. However, the contact is evidenced when reading the voltage signal, which shows a small drop at this instant. At this moment, the current is high, approximately 300 A, which easily breaks the contact between the wire and the molten pool, causing the excessive formation of fine spatter. This problem was solved by correcting the distance between the contact nozzle and the workpiece, thus eliminating one of the factors causing the instability. The distance considered ideal to prevent unwanted short-circuits and destabilization of the welding process, especially with the highest percentage of negative electrode, was 25 mm between the contact tip and the workpiece.

# 3.2 Macrographs and thermal analysis

Two samples were selected from the total number of tests for each condition, to verify the influence of the current pulses in the negative period of the wave on the bead morphology and the weld penetration profile. Figure 7 shows the cross section of the weld beads welded with different EN ratios (30, 50 and 60%) of the traditional AC waveform (Fig. 7.a) and the complex waveform, i.e., with an additional pulse in the negative phase of the wave (Fig. 7.b). It can be seen then that the weld beads produced with two AC operating conditions do not have distinct geometric characteristics. Regarding the variation of the negative percentage of the electrode, it can be seen that this did not significantly change the perspective

of the practical use of the process. Furthermore, the macrographs indicate that the heat-affected zone (HAZ) did not show a significant morphological or dimensional change.

In addition, measurements of the workpiece cooling from its bottom side were performed with a thermographic camera, immediately after the arc was extinguished. In this stage of the experiment, only a complex waveform with a negative pulse ($I_p$–, $t_p$–) and five different EN ratios (30, 40, 50, 60, 65%) were used to characterize the cooling profile of the welded part in each condition tested. The curves obtained from the cooling of the workpiece, illustrated in the graph in Fig. 8, corroborated the results previously obtained from the macrographs. It was observed that there was no significant variation in the temperature of the bottom surface of the plate for the different conditions tested, except for the curve with the lowest percentage of negative electrode (EN ratio 30%), which showed a lower cooling rate compared to the other cases. In this study, this fact is possibly attributed to the longer period in positive electrode that this percentage presents compared to the other percentages tested.

It is clear from the graph in Fig. 8 that after approximately 25 s of acquisition the sample for EN Ratio 30% assumes a cooling behavior similar to those of the other conditions with an additional alternating current pulse, reaching an average temperature of 150°C. The lowest average temperature for the conditions with pulsed alternating current was obtained for the sample with an EN ratio of 65% (142°C). This result indicates that as the percentage of negative electrode increases, the heat imposed on the workpiece, which is responsible for promoting fusion and contributes to the penetration of the weld into the base material, decreases. This can be explained by the arc length extending toward the wire electrode in the AC condition (See Fig. 4). As the arc climbs, its length and surface area increase and a greater portion of heat is dissipated to the surroundings instead of being input onto the workpiece. This ratio tends to increase as the arc becomes longer. In addition, the high convexity and height of the molten pool, (resulting in beads as seen in Fig. 8), may also be responsible for imparting heat transfer from arc to workpiece.

Although there was a maximum variation in the power value of 310 W (Table 2), the differences in the RMS currents and voltages for the various percentages of negative electrode were only 7 A and < 1 V respectively. These differences are very low considering that the object of study is AC-GMAW, a process that involves polarity changes, metal transfer across the arc, and occasional instabilities from unwanted short circuits.

Table 2
Values for the electrical signals measured during bead-on-plate welding with the complex waveform of AC-GMAW: current ($I_{Rms}$), voltage ($U_{Rms}$), wire feed speed (Wfs) and power (P)

| *Parameters* | *30% EN* | *40% EN* | *50% EN* | *60% EN* | *65% EN* |
|---|---|---|---|---|---|
| $I_{Rms}$ *(A)* | 180 | 178 | 174 | 174 | 173 |
| $U_{Rms}$ *(V)* | 24.7 | 24.8 | 24.7 | 24.7 | 23.6 |
| *Wfs* ($m.min^{-1}$) | 6.2 | 6.2 | 6.2 | 6.3 | 6.3 |
| *P (W)* | 3825 | 3807 | 3717 | 3580 | 3515 |

# 4. Conclusions

In the AC-GMAW process, the effect of negative polarity on the wire electrode was investigated. The results obtained from high-speed filming synchronized with the acquisition of the electrical signals of the welding process current and voltage allowed for the verification of aspects inherent to the behavior of the electric arc with alternating current, such as the climbing of the arc on the wire. The images obtained also contributed to a better understanding of important aspects of the AC-GMAW process, especially those related to the wire melting rate and metal transfer. In this regard, it was evidenced that there is no detachment of the metallic drop in negative polarity using a 1.2 mm diameter wire, although a high intensity current pulse is employed for a short period of time. No extinguishing of the arc during polarity reversal was detected, which can be observed in other arc welding processes when using alternating current This result suggests that a current pulse at the end of the negative time, just before the positive current pulse, contributed primarily to arc stiffness and stability. The waveform associated with a high current intensity pulse during the negative polarity did not promote significant differences in the bead morphology and weld penetration profile compared to the traditional AC-GMAW waveform used. In a complementary way, and supporting the other results obtained, the thermographic analysis showed that as the negative electrode ratio increased, the dynamic temperature behavior suffered only slight impact, showcasing a slower cooling rate for the lower EN Ratio tested (30%), whereas no appreciable difference was noted after 40 s from weld end. Thus, according to the results obtained, a high-intensity current pulse in negative polarity in this AC wave variant acts as a tool for preheating the molten pool, increasing the melting rate of the wire abruptly and stiffening the arc during the polarity change.

# Declarations


## Funding

This work was supported by the Brazilian governmental agencies: Coordenação de Aperfeiçoamento de Pessoal de Nível Superior - Brazil (CAPES) and Conselho Nacional de Desenvolvimento Científico e Tecnológico - Brazil (CNPQ).

### Competing interests

The authors have no relevant financial or non-financial interests to disclose.

### Availability of data and material (data transparency)

Not applicable

### Code availability (software application or custom code)

Not applicable

### Ethics approval (include appropriate approvals or waivers)

Not applicable

### Consent to participate (include appropriate statements)

Not applicable

### Consent for publication (include appropriate statements)

Not applicable

### Authors' contributions

All authors contributed to the study conception and design. Material preparation, data collection and analysis were performed by Álisson Fernandes da Rosa, Luciano Machado Cirino, Claudio Marques Schaeffer, Mateus Barancelli Schwedersky and Régis Henrique Gonçalves e Silva. The first draft of the manuscript waswritten by Álisson Fernandes da Rosa and all authors commented on previous versions of the manuscript. All authors read and approved the final manuscript.

# References


1. Essers WG, Van Gompel MM (1984) Arc control with Pulsed GMAW Welding. **Welding Journal**, Miami, v. 6, p.26–32
2. Dutra JC, Silva e, Savi RHG, Marques BM, Alarcon C (2016) O. E. New methodology for AC-pulsed GMAW parameterization applied to aluminum shipbuilding. **Journal of the Brazilian Society of Mechanical Sciences and Engineering**, 38(1), 99–107. http://dx.doi.org/10.1007/s40430-015-0351-3
3. Kah P, Suoranta R, Martikainen J (2013) Advanced gas metal arc welding processes. **The International Journal of Advanced Manufacturing Technology**, 67(1), 655–674. http://dx.doi.org/10.1007/s00170-012-4513-5
4. Cary HB (1988) Modern Welding Technology 2th Ed. Prentice-Hall, Inc
5. Talkington JE (1998) Variable polarity gas metal arc welding. The Ohio State University

6. Kim K, Chung H (2017) Wire melting rate of alternating current gas metal arc welding. **The International Journal of Advanced Manufacturing Technology**, 90(5–8), 1253–1263. http://dx.doi.org/10.1007/s00170-016-9384-8
7. Souza D, Resende AAD, Scotti A (2009) Um modelo qualitativo para explicar a influência da polaridade na taxa de fusão no processo MIG/MAG. **Soldagem & Inspeção**, 14. 192–198. http://dx.doi.org/10.1590/S0104-92242009000300002. 3
8. Dutra JC, Silva e, Marques RHG, Viviani C (2016) A. B. A new approach for MIG/MAG cladding with Inconel 625. **Welding in the World**, 60(6), 1201–1209. https://doi.org/10.1007/s40194-016-0371-3
9. Yarmuch MAR, Patchett BM (2007) Variable AC polarity GTAW fusion behavior in 5083 aluminum. Weld J 86(7):196
10. Tong H, Ueyama T, Harada S, Ushio M (2001) Quality and productivity improvement in aluminium alloy thin sheet welding using alternating current pulsed metal inert gas welding system. **Science and Technology of Welding and joining**, vol. 6, 203–208. https://doi.org/10.1179/136217101101538776
11. ROSA et al., Root Opening Performance and Geometric Weld Features in GMAW-AC. **Welding Journal**, v. 101, n. March, p. 62–67
12. HARWIG DD (2003) Arc Behavior and Metal Transfer in VP-GMAW Process. Cranfield University – School of Industrial and Manufacturing Science
13. Joseph A, Webb C, Haramia M, Yapp D (2003) Variable polarity (AC) arc weld brazing of galvanized steel. **In**: **IIW INTERNATIONAL CONFERENCE**, Bucharest. Proceedings of 56th IIW International Conference. p. 1–10
14. Arif N, Chung H (2015) Alternating current-gas metal arc welding for application to thick plates. J Mater Process Technol 222:75–83. http://dx.doi.org/10.1016/j.jmatprotec.2015.02.041
15. Dutra JC, e Silva RHG, Savi BM, Marques C, Alarcon OE (2016) New methodology for AC-pulsed GMAW parameterization applied to aluminum shipbuilding. **Journal of the Brazilian Society of Mechanical Sciences and Engineering**, 99–107. https://doi.org/10.1007/s40430-015-0351-3
16. IKRAM A, RAZA A, CHUNG H (2020) Investigation of Single Pass Welding of Thick AH36 Steel Plates in a Square Groove Butt Joint Configuration During AC-GMAW. **Journal of Welding and Joining**, v. 38, n. 3. 254–262. https://doi.org/10.5781/JWJ.2020.38.3.4
17. Kang S, Kang M, Jang YH, Kim C (2020) Droplet transfer and spatter generation in DC–AC pulse tandem gas metal arc welding. Sci Technol Weld Joining 25(7):589–599. https://doi.org/10.1080/13621718.2020.1786262
18. Zhang YM, Yang YP, Zhang W, Na SJ (2020) Advanced welding manufacturing: a brief analysis and review of challenges and solutions. J Manuf Sci Eng 142(11). https://doi.org/10.1115/1.4047947
19. HONG SM et al (2021) Numerical analysis of the effect of heat loss by zinc evaporation on aluminum alloy to hot-dip galvanized steel joints by electrode negative polarity ratio varied AC pulse gas metal arc welding. **Journal of Manufacturing Processes**, v. 69, n. 4, p. 671–683. https://doi.org/10.1016/j.jmapro.2021.08.019

20. ARIF N, CHUNG, H (2014) Alternating current-gas metal arc welding for application to thin sheets. **Journal of Materials Processing Technology**, v. 214, n. 9. 1828–1837. http://dx.doi.org/10.1016/j.jmatprotec.2014.03.034
21. Jaskulski K (2010) Robotyzacje OTC z wykorzystaniem niskoenergetycznych metod spawania. Available at: https://docplayer.pl/14052107-Robotyzacje-otc-z-wykorzystaniem-niskoenergetycznych-metod-spawania.html. Accessed on: 07 April, 2021
22. OTC Daihen, Owner's Manual / Model Digital Inverter DW-300. https://www.otc-daihen.de/index.php?id=2581
23. Vilarinho LO, Nascimento AS, Fernandes DB, MOTA CM(2009) Methodology for parameter calculation of VP-GMAW. **Welding Journal**, vol. 88, n. 4, p. 92–98
24. SCOTTI A, MONTEIRO LS (2012) Uma metodologia para parametrização do processo MIG/MAG CA. **Soldagem & Inspeção**, v. 17, n. 3. 271–277. http://dx.doi.org/10.1590/s0104-92242012000300011
25. Park HJ, Kim DC, Kang MJ, Rhee S(2013) The arc phenomenon by the characteristic of EN ratio in AC pulse GMAW. **The International Journal of Advanced Manufacturing Technology**, 66(5–8), 867–875. http://dx.doi.org/10.1007/s00170-012-4371-1
26. SCOTTI A, PONOMAREV V (2008) Soldagem MIG/MAG: Melhor Entendimento Melhor Desempenho. Artliber, São Paulo

# Figures

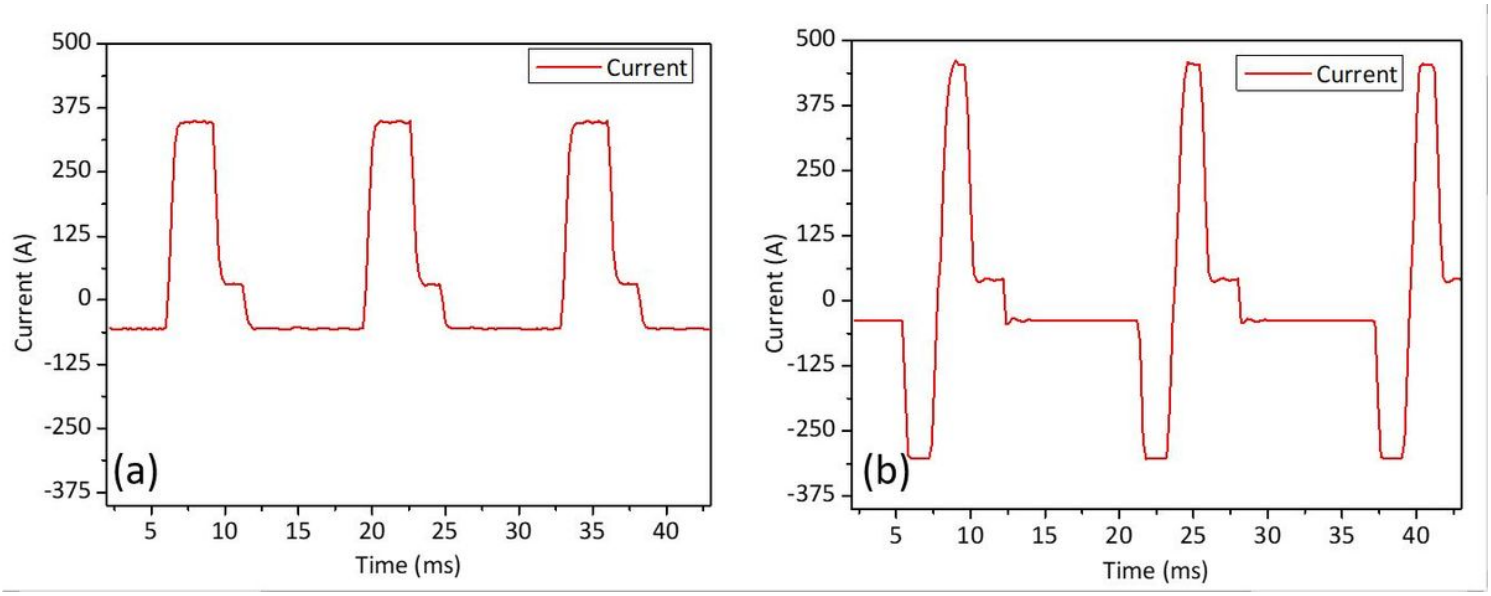


**Figure 1**

Examples of the welding current waveforms: (a) traditional AC-GMAW welding processes and (b) complex waveform of AC-GMAW with two plateaus in negative polarity

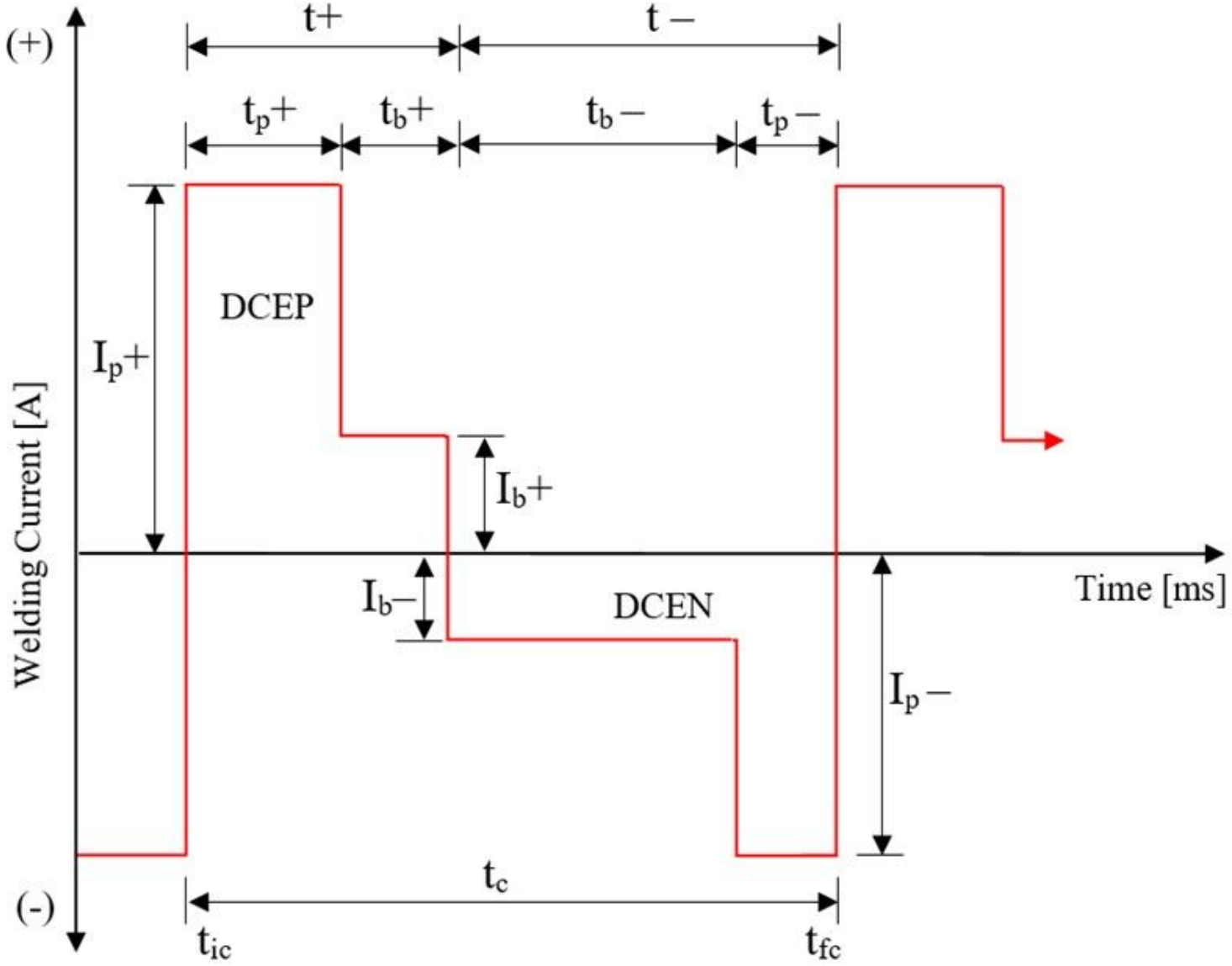


**Figure 2**

Current waveform thresholds

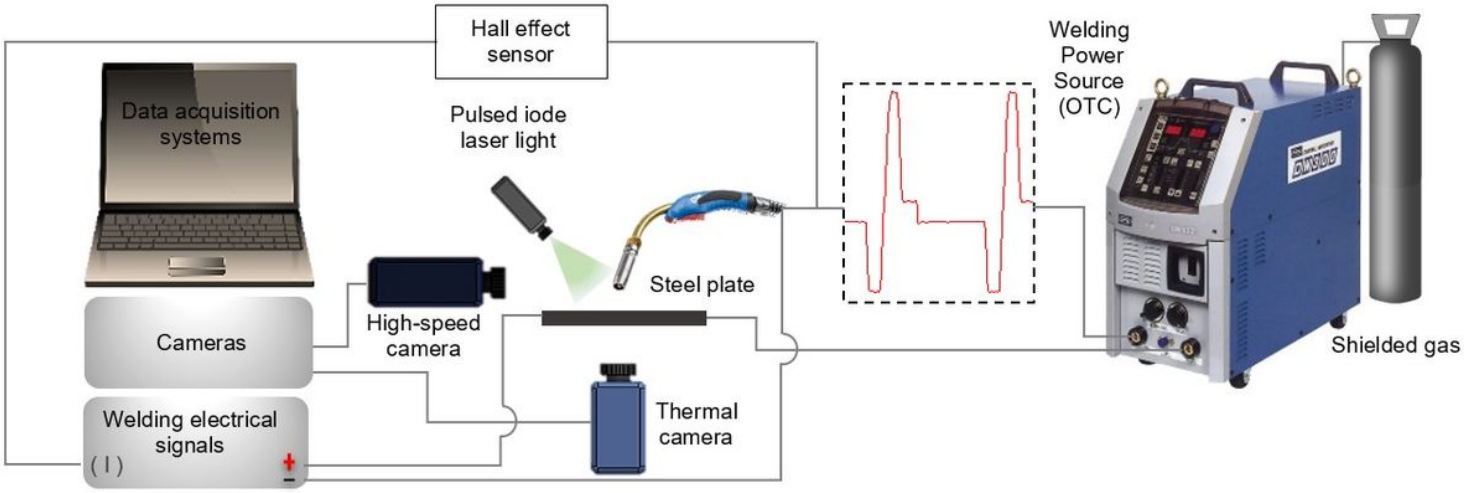

## Figure 3

Schematic diagram of the welding experiment

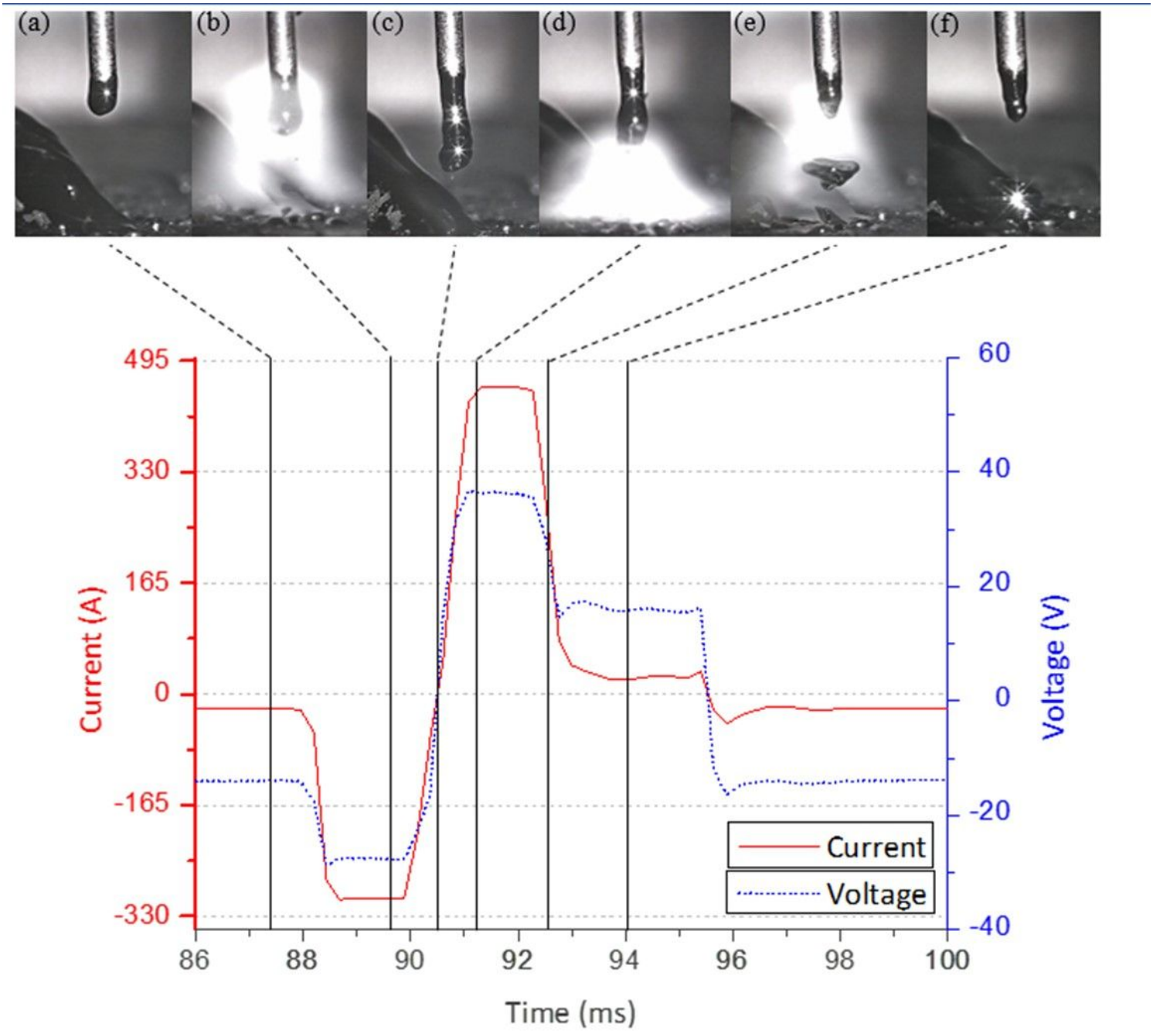


## Figure 4

Waveform and metal transfer in the AC-GMAW process using negative pulse: EN ratio 60% and wire feed speed 6.2 $m.min^{-1}$ (videos are available as supplement material)

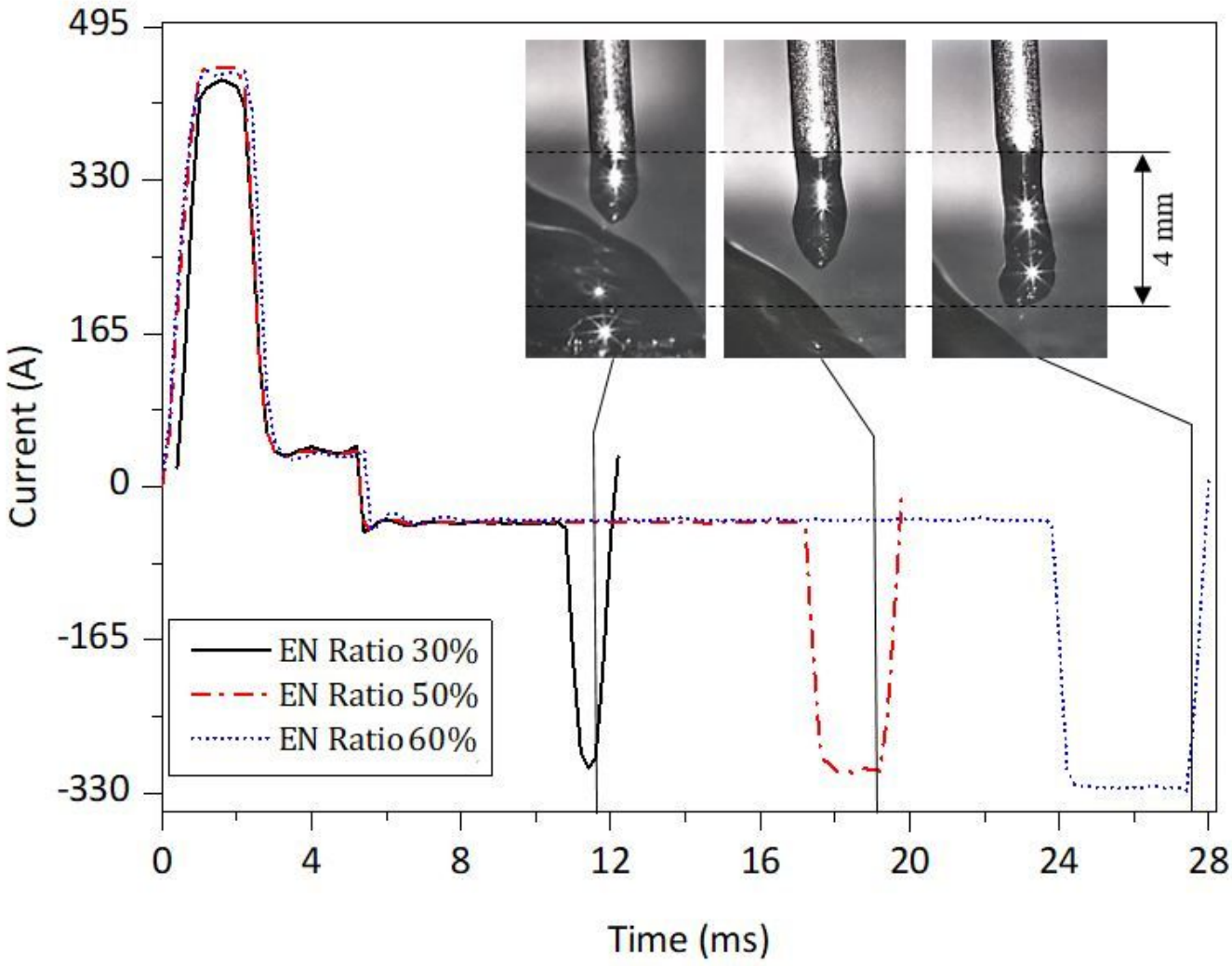


**Figure 5**

Overlapping current curves of complex waveform of the AC-GMAW process

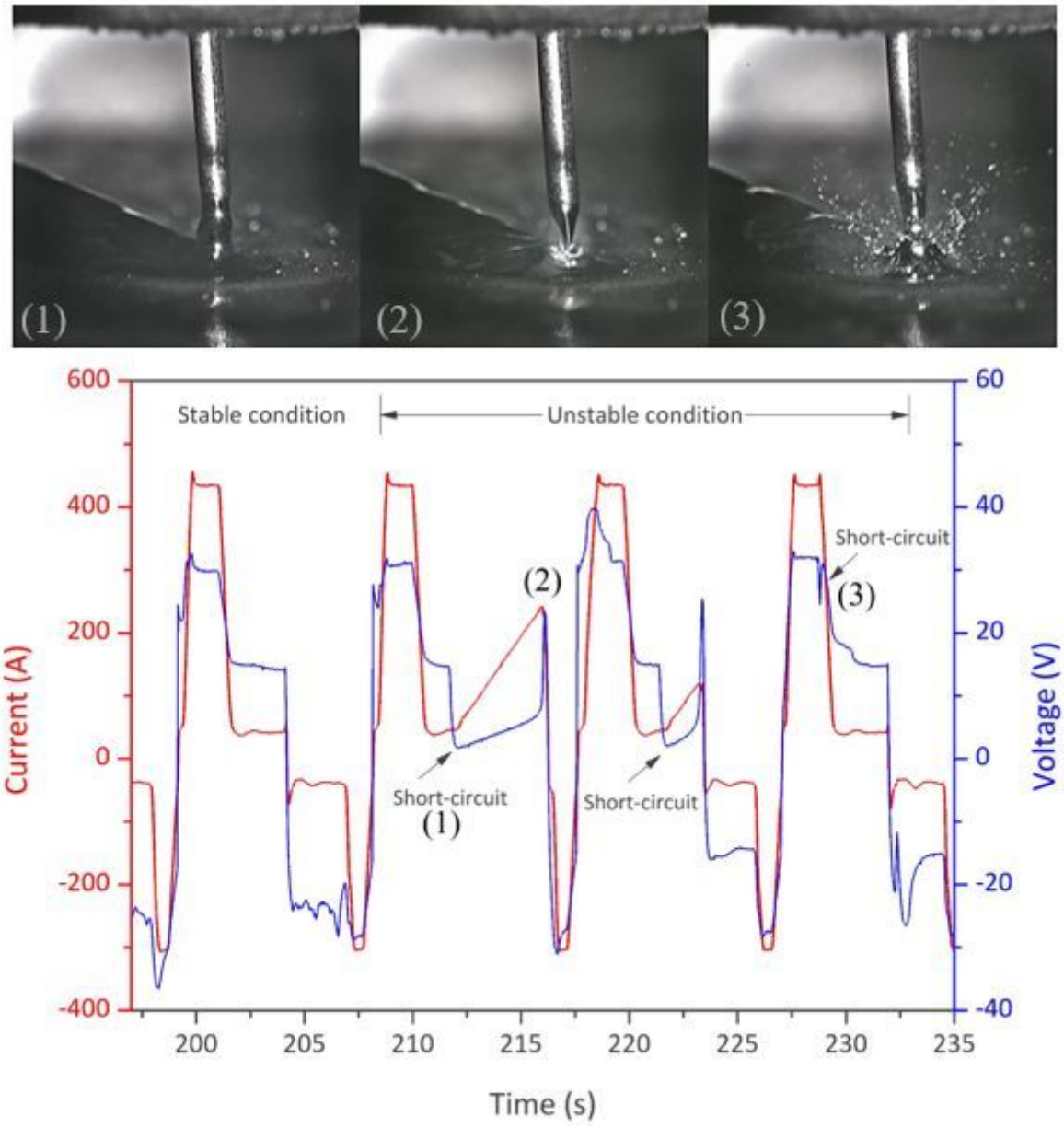


## Figure 6

Unfavorable wire electrode contact and effect on the stability of the electrical signals obtained with high percentage of negative electrode (videos provided as supplement material)

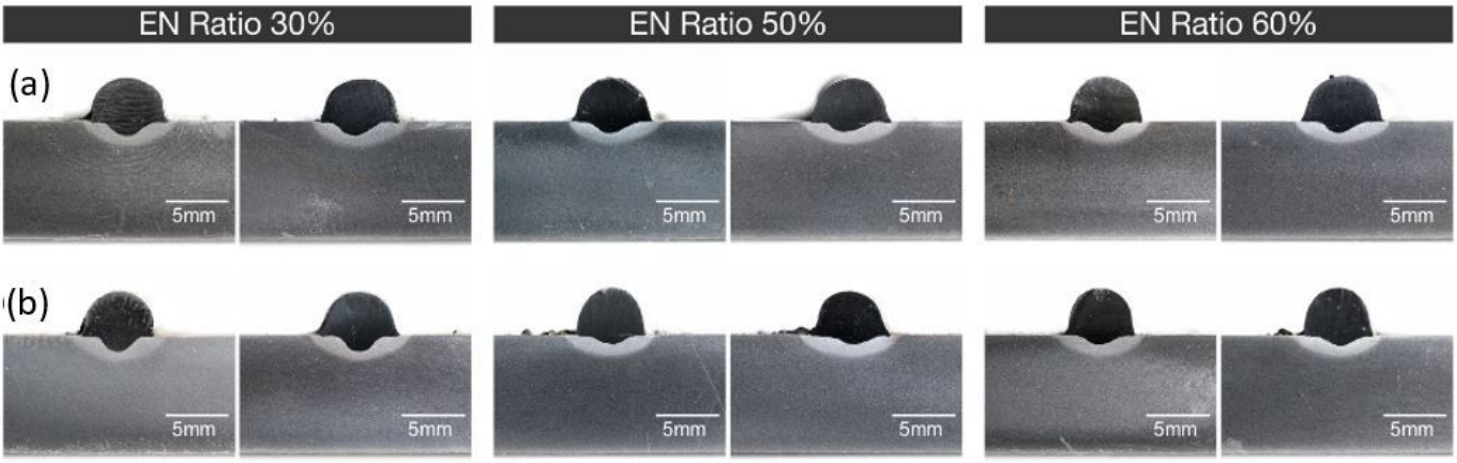


**Figure 7**

Comparison of the cross section of weld beads obtained with the AC-GMAW process: (a) traditional AC-GMAW and (b) complex waveform of AC-GMAW

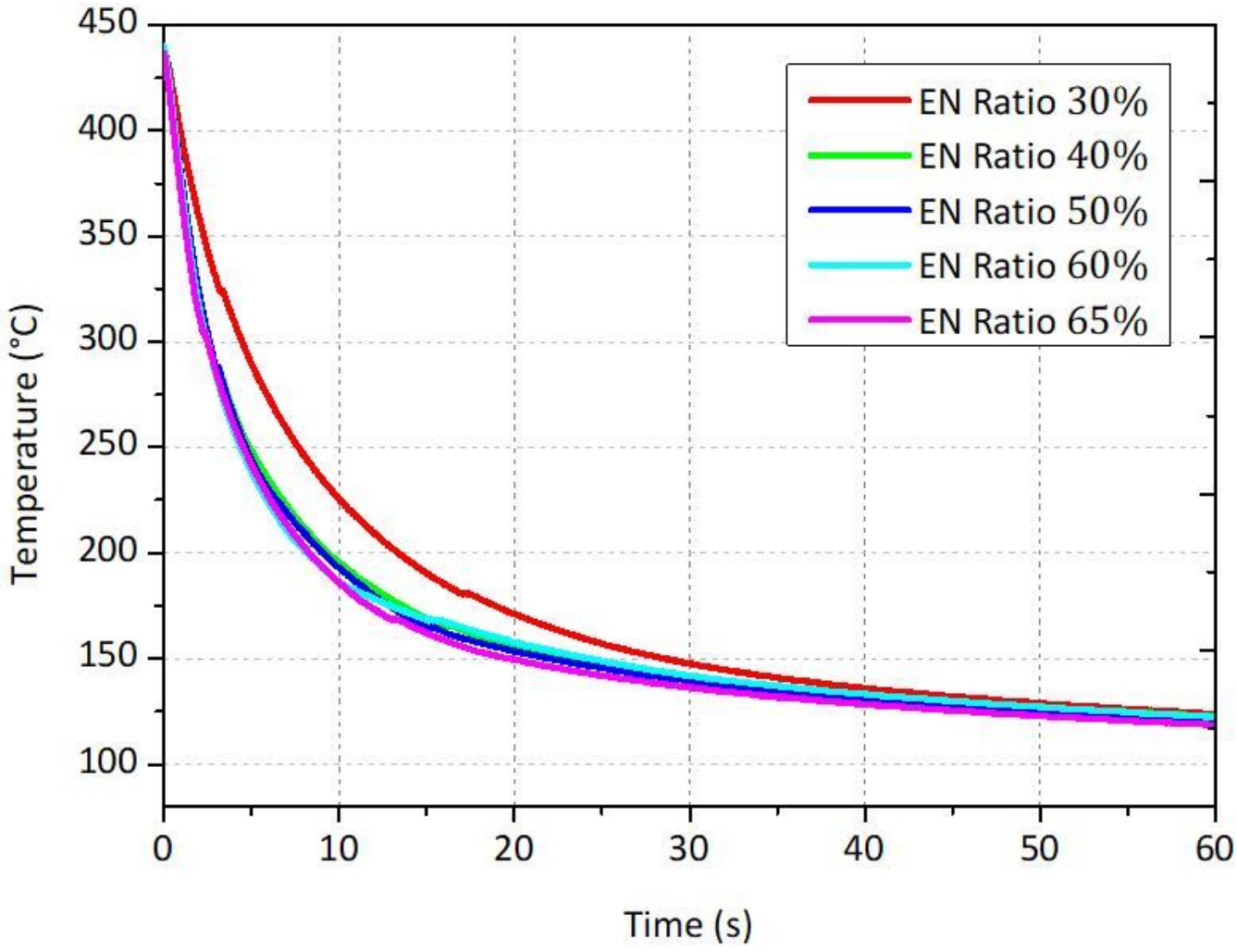


**Figure 8**

Cooling time obtained from thermal filming of the back of the steel plates

## Supplementary Files

This is a list of supplementary files associated with this preprint. Click to download.

- VideoFigure4.mp4